Flow Field Characteristics of Translating and Revolving Flexible Wings

Perçin, Mustafa; Yazdanpanah, Mahdi; Amiri, Human; van de Meerendonk, Remco; van Oudheusden, Bas

Important note
To cite this publication, please use the final published version (if applicable).
Please check the document version above.

Flow Field Characteristics of Translating and Revolving Flexible Wings

Mustafa Percin[1*], Mahdi Yazdanpanah[1], Human Amiri [2], Remco van de Meerendonk[3], B.W. van Oudheusden[3]

[1] Middle East Technical University, Department of Aerospace Engineering, 06800 Ankara, Turkey

[2] METU center for Wind Energy, 06800 Ankara, Turkey

[3] Delft University of Technology, Faculty of Aerospace Engineering, Delft, The Netherlands

[*] mpercin@metu.edu.tr

Abstract

This study explores the effects of rotational mechanisms on the characteristics of the leading edge vortex (LEV) by comparing translating and revolving flexible wings that are started from rest. Tomographic particle image velocimetry (tomographic-PIV) technique was employed to acquire three-dimensional flow fields for the revolving wings, while planar flow fields for the case of translating wings were acquired via 2D2C-PIV measurements. The comparison of flow fields between the two motion kinematics reveals similar behavior of the vortical structures yet the LEV circulation in the translating wings has higher values. The LEV centroid in the revolving cases stays above the leading-edge, while in the translating wings, it always remains at a lower position. The effect of high flexibility results in the retention of LEV closer to the wing surface for both cases.

1 Introduction

Nature has been a great source of inspiration in the design and development of flying machines for centuries. Recently, with the advent of micro air vehicles (MAVs), many researches focus on the flapping flight of biological flyers since other means of flight (i.e., fixed wing and rotary wing) become inefficient in the typical low Reynolds number (Re) regime of MAV operation (Pines and Bohorquez, 2006).

Flapping flight is an unsteady three-dimensional phenomenon, where the generation of a stable leading-edge vortex (LEV) has shown to be one of the most prominent force generation mechanisms. (Sane SP, 2003). It has been subject to numerous investigations, and different hypotheses have been put forward regarding its stability, such as spanwise advection of vorticity (Ellington et al., 1996), tip vortex inducing a downward flow and inhibiting the growth of the LEV, (Birch and Dickinson, 2001) or the apparent rotational (Coriolis and rotational) accelerations in the low Rossby number regime (Lentink and Dickinson, 2009). The latter hypothesis has also been supported by the studies of Jardin and David (2014, 2015), where they showed that the enhanced aerodynamic performance is ensured by the apparent Coriolis effect while the LEV attachment can be achieved by the spanwise advection of vorticity.

The flapping wing motion can be decomposed into three motion kinematics: sweeping, plunging and pitching. In the literature, the sweeping motion is simulated by either a rectilinear translation (i.e., infinite Rossby number) or revolving motion (finite Rossby number). The latter is a more realistic

representation of the actual case due to the occurrence of rotational accelerations, which, as aforementioned, are considered to be responsible for the prolonged attachment of the LEV.

Flapping-wing phenomena in realistic configurations is further complicated by the presence of wing flexibility, which is an aspect often disregarded in mechanical simulations. Different studies have revealed possible benefits of wing flexibility on the aerodynamic performance (Shyy et al., 2010). Zhao et al. (2010) showed that flow structures are similar for different wing flexibilities yet the size of the LEV is influenced by the flexural stiffness. Beals and Jones (2015) considered a revolving motion of a chordwise-flexible wing in the Re range of from 10,000 to 25,000. Lift is significantly lower for the flexible wing, yet the wing deformation mitigated the negative effects of the wake encounter.

The main objective of this study is to investigate the effects of rotational mechanisms that are responsible for the stability of the LEV for chordwise-flexible wings, by comparing the flow fields when the wings are undergoing translational (rectilinear) or revolving (curvilinear) motions. Three different flexural stiffness values (rigid, moderate flexibility and high flexibility) are considered. Force and tomographic particle image velocimetry (tomographic-PIV) measurements were performed on the revolving wings (van de Meerendonk et al., 2018). Flow field measurements via 2D-PIV technique were conducted for the translating wings case.

2   Experimental methods

Both motion kinematics (revolving and translating) include an acceleration phase and a constant speed phase. The wing begins to revolve (translate) from rest, and it moves with constant acceleration until it reaches the predefined terminal velocity (V_t) over one chord length of travel (δ^*=1), which for the revolving wing is measured at the 75% span location. Subsequently, the wing continues its motion at this velocity up to more than four chord lengths of travel. The value of V_t is 0.2 m/s for the revolving experiment and 0.08 m/s for the translating-wing experiments, the different values being a consequence of the different restrictions of the two setups. However, the wing dimensions are scaled accordingly in order to achieve equivalent values of the stiffness parameter.

Three wing models with different flexural stiffness values were considered for the tests. A virtually rigid wing is built from 1 mm thick Plexiglas, whereas the moderately flexible and highly flexible wings are built from Polyethylene terephthalate (PET) with thickness values of 175 μm and 125 μm, respectively. For the revolving wing experiments, the model is a rectangular flat plate with a chord length (c) of 50 mm and a span length of 100 mm, while for the translating wing experiments the model has a chord length (c) of 92 mm and a span length of 184 mm. In both cases, the wing aspect ratio is 2. The corresponding Reynolds number for the revolving and translating wing experiments are 10,000 and 7,360, respectively. The relative insensitivity of the flow structures to Reynolds number in this flow regime (Percin and van Oudheusden, 2015) allows for a proper comparison between the two tested motion kinematics. Bending stiffness parameter (Π), which describes the ratio between the elastic bending forces and the fluid-dynamic forces is as follows (Shyy et al., 2010):

$$\Pi_1 = \frac{Eh^3}{12(1-\upsilon^2)\rho V_t^2 c^3} \, , \tag{1}$$

where υ is the Poisson ratio, E is Young's modulus, h is thickness value, and V_t is terminal velocity. In the bending stiffness parameter equation, a Poisson ratio (υ) of 0.4 for Plexiglas and PET is considered. 1000 (kg/m³) is taken for the density of water. The dimensions of translating wings are calculated to have the same stiffness parameters as the revolving wings have. The material properties of the wing models are reported in Table 1.

Material	Description	Young's modulus $E\ [Nm^{-2}]$	Thickness h $[mm]$	Bending stiffness parameter Π_1
Rigid	Plexiglas	$\approx 3300 \cdot 10^6$	1	65.5
Moderate flexibility	PET	$\approx 4350 \cdot 10^6$	0.175	0.46
High flexibility	PET	$\approx 4500 \cdot 10^6$	0.125	0.17

Table 1: Model properties

The revolving-wing experiments were performed in an octagonal water tank (Fig. 1) at the Aerodynamics Laboratory of Delft University of Technology (TUD) (van de Meerendonk et al., 2018). The translating wing experiments were performed in an octagonal water tank at the Aerospace Engineering Department of Middle East Technical University (METU). The dimensions of the tank are 1 m × 1.5 m (distance between parallel edges × height) and the wing models are driven in the tank by a robotic arm having three degrees of freedom (translation in the x and y-axes and 360° of rotation around the pitching axis of the wing model). PIV cameras are placed on the camera board, which is connected to robotic arm, and it moves with the robotic arm. Thus the flow field and leading-edge positions in all images are same. Experimental setup for the translating-wing experiments is shown in Fig. 2. The 2D-PIV setup is composed of a double-pulse Nd: YAG laser at a wavelength of 532 nm with a pulse energy of 120 mJ and two 12-bit HiSense MkII CCD cameras placed side-by-side in order to increase the field of view to 247.5 mm × 143.9 mm. The corresponding magnification factor is 0.059. The PIV Images from two cameras were stitched according to the mapping information obtained before the PIV measurements. The double-frame images were cross-correlated using interrogation areas of 64 × 64 pixel² with 75% of overlap. The universal outlier detection technique (Westerweel and Scarano, 2005) was applied to the cross-correlation results to detect and substitute the unreliable velocity vectors. Finally, for each phase the velocity fields were ensemble averaged in order to increase the signal to noise ratio.
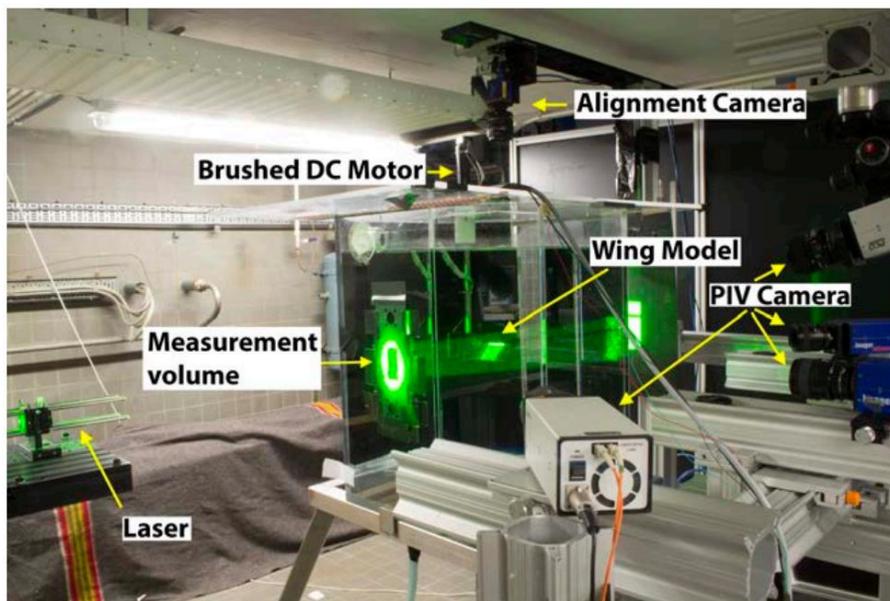

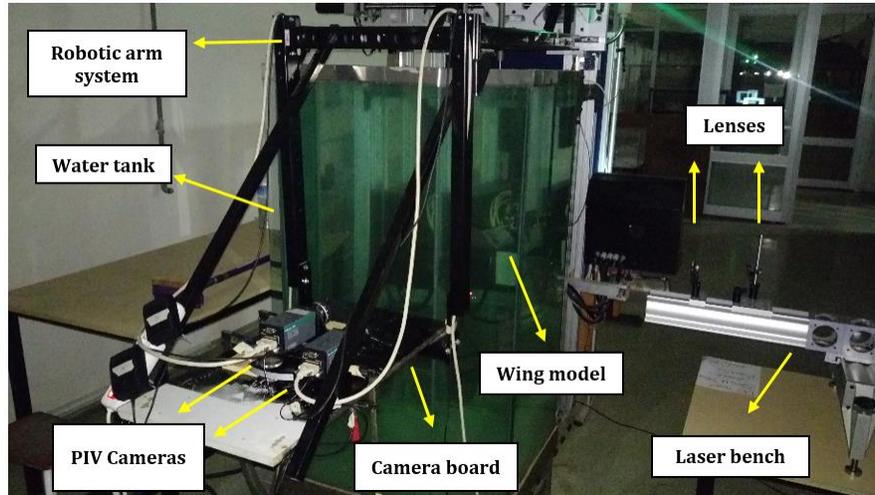Figure 1: Tomographic PIV setup for revolving-wings experiments.

Figure 2: 2D-PIV setup for translating-wing experiments.

3 Results and discussion

The out-of-plane vorticity contours at the 75% span position for δ^*= 1.0, 1.5, 2, and 4 for the translating and revolving flexible wings are shown in Fig. 3, respectively. The out of plane vorticity contours suggest similar vortex formations: a coherent LEV and a train of trailing edge vortices particularly at the initial phases of both motion kinematics and a chaotic flow field with an elongated incoherent positive vorticity layers emanating from the leading edge at a later phase (δ^*= 4). At the end of the acceleration phase for both motions (δ^*= 1), a lifted off fragmented LEV is present in the flow fields, which is in accordance with those reported in the literature (Percin and van Oudheusden, 2015). In the subsequent stages, the behavior of the LEV is similar for both motion kinematics, yet the LEV circulation value is slightly higher in the case of the translating wing, as shown in Fig. 4. At δ^*= 4, the coherent LEV is burst into small-scale structures in both translating and revolving wings. Particularly in the case of rigid and moderately flexible wings, the shear layers emanating from the leading and trailing edges interact, and this interaction leads to small-scale vorticity pockets populating the wake. For the translating rigid and moderately flexible wings, the flow is completely detached from the wing surface, however, for the highly flexible wing, the flow that separates at the leading edge reattaches to the wing surface slightly before the trailing edge. This may be attributed to the decreased effective angle of attack of the highly flexible wing due to relatively higher deformation.
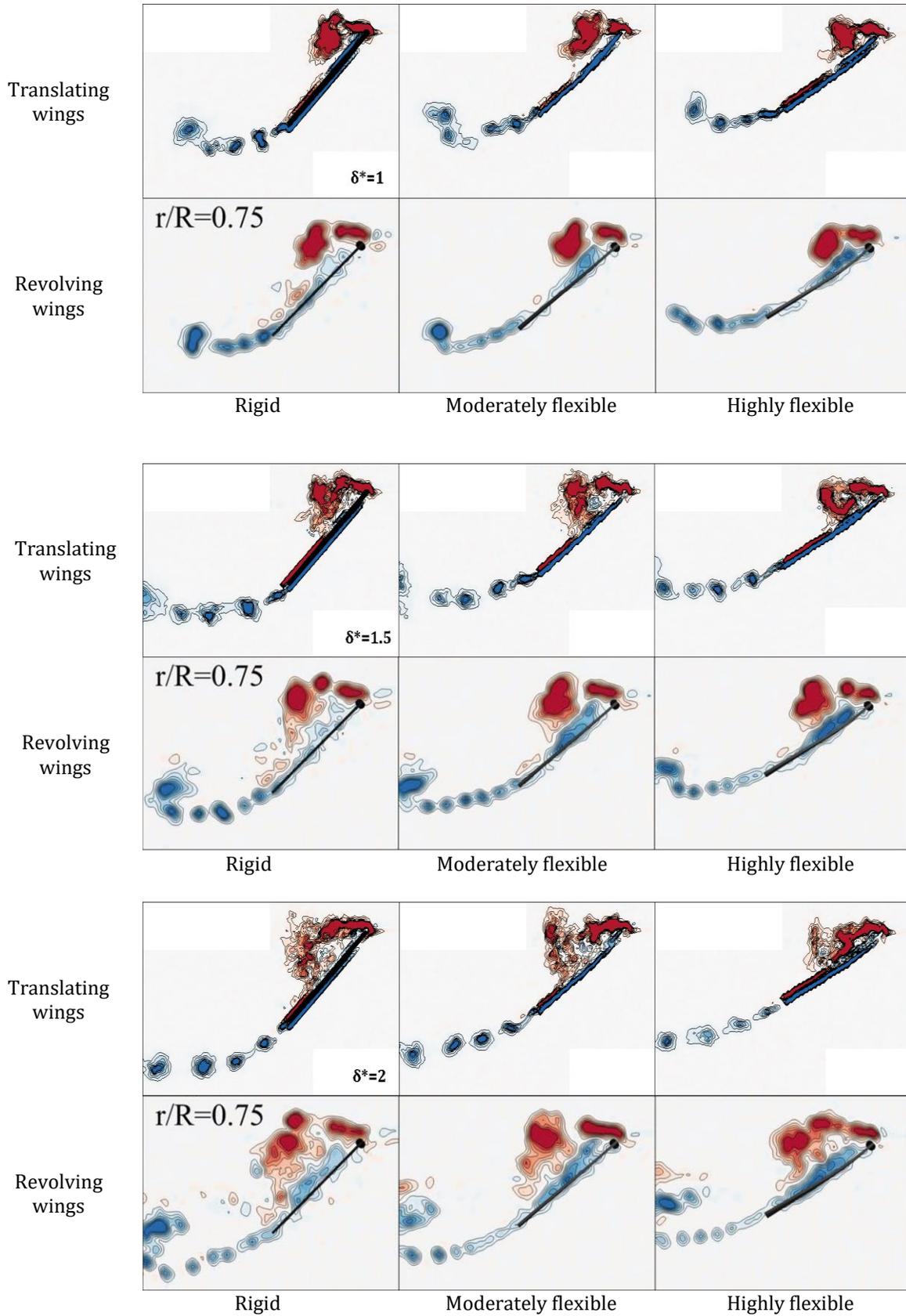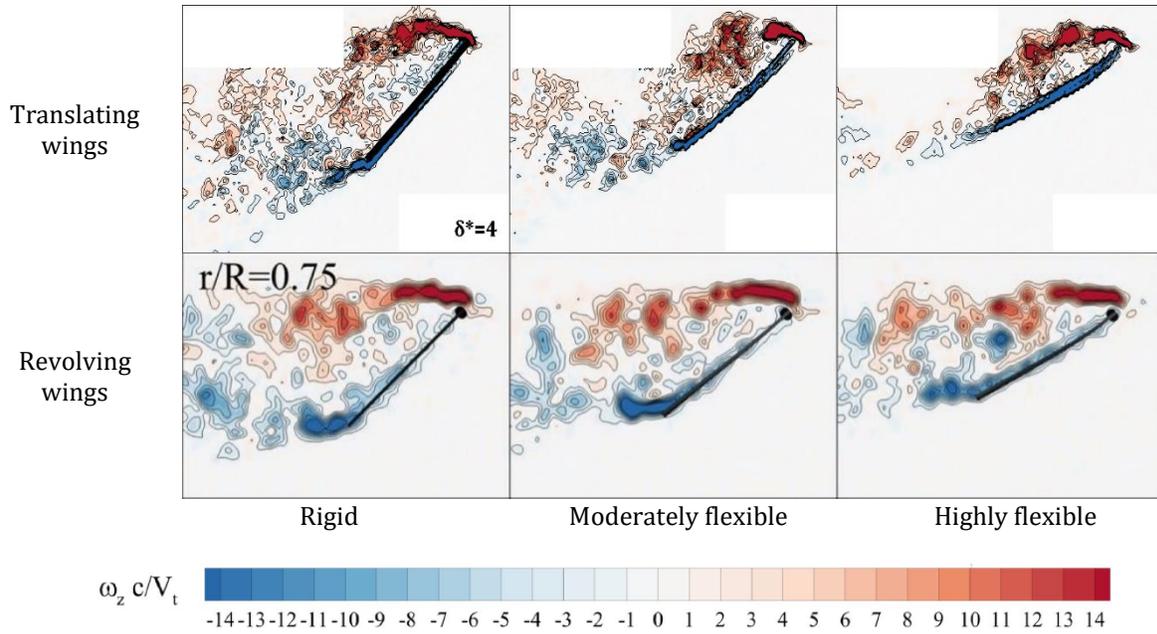
Figure 3: The out-of-plane vorticity contours for δ^*= 1.0, 1.5, 2, and 4 with respect to the 75% span position

There are two prominent differences between the translating and revolving wings in terms of the normalized LEV circulation values. First, the translating motion yields greater circulation values. Second, the LEV circulation stays higher after δ^*= 3 compared to the revolving wing case. However, this may be due to the shortcoming of the vortex core detection strategy in the detection of the LEV boundaries.
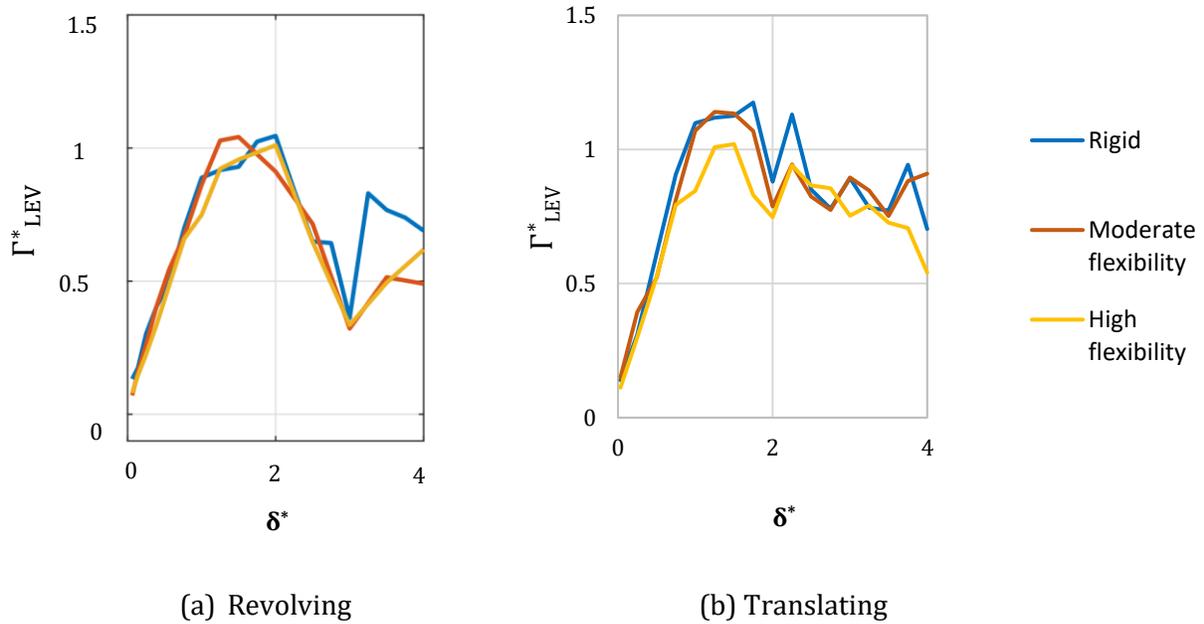

(a) Revolving

(b) Translating

Figure 4: Temporal evolution of LEV circulation (Γ^*_{LEV}) for translating and revolving wings.

In Fig.5, the temporal evolution of the LEV in x and y directions are shown for translating (right side) and revolving wings (left side).

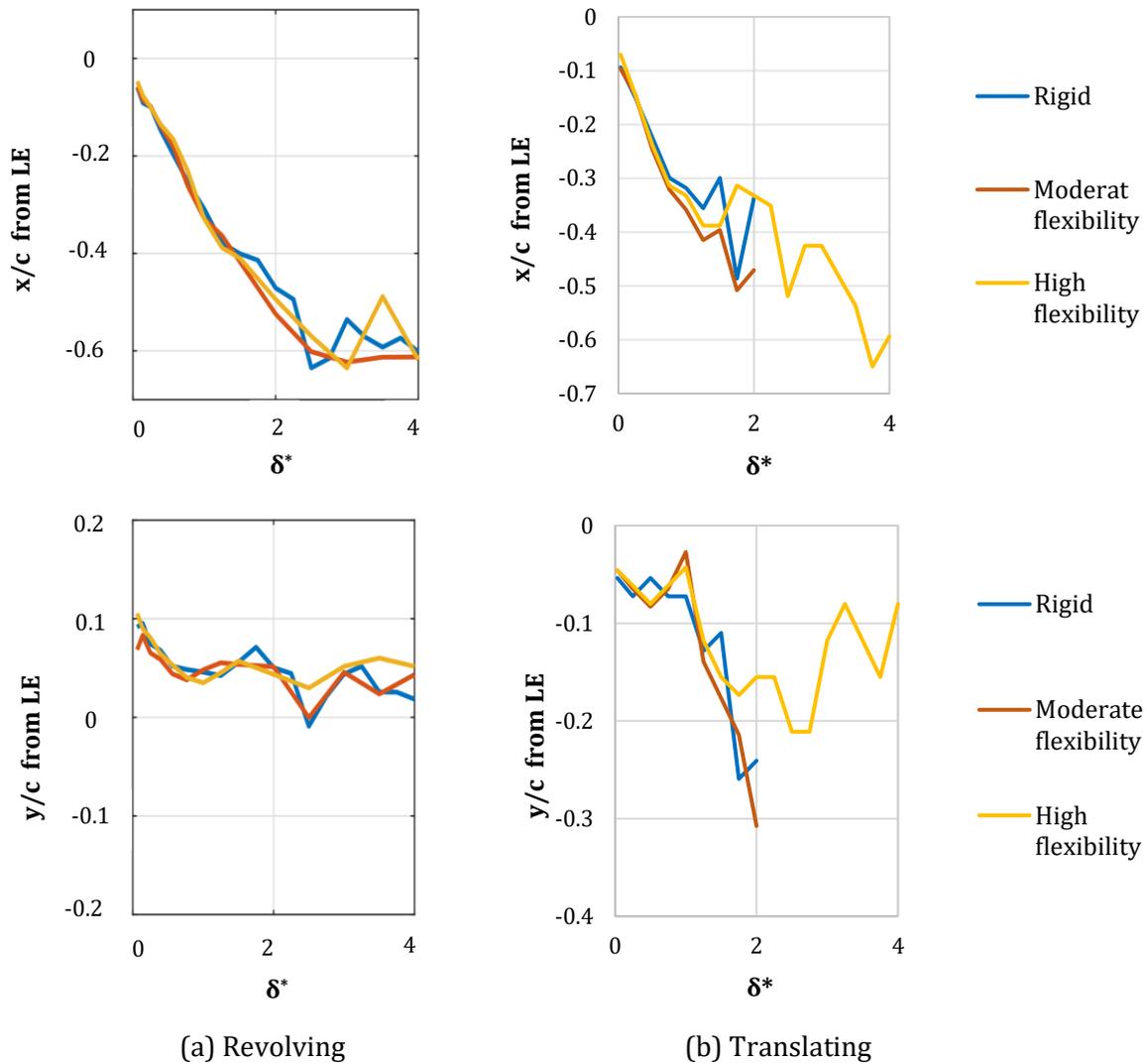(a) Revolving   (b) Translating

Figure 5: Temporal evolution of the LEV centroid. Top: Chord distance in x-direction from LE. Bottom: Chord distance in y-direction from the LE.

The temporal evolution of the LEV centroid also displays a similar trend for both motion kinematics (Fig. 5). The major difference in this respect is that the LEV stays at a lower location (y/c) with respect to the leading edge and continuously move away in the vertical direction in the case of the translating wing while it stays at a more-or-less fixed location in the case of the revolving wing.

Conclusions

The flow characteristics of rigid and flexible wings undergoing revolving and translating motions were investigated in this study. Three-dimensional flow fields were acquired by the use of tomographic-PIV for the revolving wings and planar flow fields were studied by employing 2D2C PIV for the translating wings. LEV characteristics in both motion kinematics was explored. Similar vortex

formations and vorticity clusters at the initial phases and similar chaotic flow fields at subsequent phases are observed for both motion kinematics. The behavior of LEV is similar for both motions; however, the LEV circulation is shown to be slightly higher in the translating motion. Although the flow is detached from the wing surface in the translating rigid and moderately flexible wings at the late phases of the motion, it reattaches to the wing surface in the highly flexible wing. The LEV is burst in the translating rigid and moderately flexible wings after two chord lengths of travel; however, the LEV in the highly flexible wing keeps its coherency due to the deflection of the wing and thus smaller effective angle of attack. The LEV rises and stays at a higher position with respect to the leading-edge in the revolving wings, while in the translating wings, it always stays at a relatively lower position.

References

Beals N, and Jones AR (2015) Lift Production by a Passively Flexible Rotating Wing. *AIAA Journal* 53:10

Birch JM, and Dickinson MH (2001) Spanwise flow and the attachment of the leading-edge vortex on insect wings. *Nature* 412:6848

Ellington CP, Van Den Berg C, Willmott AP, and Thomas AL (1996) Leading-edge vortices in insect flight. *Nature* 384:6610

Jardin T, and David L (2014) Spanwise gradients in flow speed help stabilize leading-edge vortices on revolving wings. *Physical Review E* 90:1

Jardin T, and David L (2015) Coriolis effects enhance lift on revolving wings. *Physical Review E* 91:3

Lentink D, and Dickinson MH (2009) Rotational accelerations stabilize leading edge vortices on revolving fly wings. *Journal of Experimental Biology* 212:16

Percin M, and van Oudheusden BW (2015) Three-dimensional flow structures and unsteady forces on pitching and surging revolving flat plates. *Experiments in Fluids* 56:47

Pines DJ, and Bohorquez F (2006) Challenges Facing Future Micro-Air-Vehicle Development. *Journal of Aircraft* 43:2

Sane SP (2003) The aerodynamics of insect flight. *Journal of Experimental Biology* 206:23

Shyy W, Aono H, Chimakurthi SK, Trizila P, Kang CK, Cesnik CE, and Liu H (2010) Recent progress in flapping wing aerodynamics and aeroelasticity. *Progress in Aerospace Sciences* 46:7

van de Meerendonk R, Percin M, and van Oudheusden BW (2018) Three-dimensional flow and load characteristics of flexible revolving wings. *Experiments in Fluids* 59:161

Westerweel J, and Scarano F (2005) Universal outlier detection for PIV data. *Experiments in Fluids* 39: 1096

Zhao L, Huang Q, Deng X, and Sane SP (2010) Aerodynamic effects of flexibility in flapping wings. *Journal of The Royal Society Interface* 7:44